Bull. Soc. R. Sci. Liège, 2024, **93**(2), 582–588 *Peer-reviewed conference paper*
doi:10.25518/0037-9565.11805

Extraction of YSO Cores and Active Regions near the Star-forming Site AFGL 5157

Aayushi VERMA[1,*], Saurabh SHARMA[1] and Lokesh DEWANGAN[2]

[1] Aryabhatta Research Institute of observational sciencES (ARIES), Manora Peak, Nainital–263001, India

[2] Physical Research Laboratory, Navrangpura, Ahmedabad–380 009, India

[*] Corresponding author: aayushiverma@aries.res.in

Paper presented at the 3rd BINA Workshop on "Scientific Potential of the Indo-Belgian Cooperation", held at the Graphic Era Hill University, Bhimtal (India), 22nd–24th March 2023.

Abstract

We have carried out a quantitative analysis of the $1^\circ \times 1^\circ$ region near star-forming site AFGL 5157 using *'Minimal Spanning Tree'* (MST). The analysis reveals that this region consists of five major clusters. The cluster radii of the cores and active regions were found to be varying between 0.75–2.62 pc and 2.77–4.58 pc, respectively, for these regions, while the aspect ratio varies between 0.71 to 7.17. This hints towards the clumpy as well as elongated clusters in the region. We calculated structure parameter Q for each region which varies between 0.41–0.62 and 0.23–0.81 for the cores and ARs, respectively. This shows the existence of fractal distribution in all the cores and ARs except the core of the [HKS2019] E70 bubble.

Keywords: Interstellar medium, Star formation, Star-forming regions

1. Introduction

The formation of stars occurs in a group of clusters and associations, and it is assumed that they cannot be formed in isolation (Lada and Lada, 2003). Observational analyses of embedded star-forming regions reveal that the distribution of stars is generally elongated, clumpy, or both (Allen et al. 2008; Koenig et al. 2008). This distribution is correlated with the distribution of dense molecular gas of natal clouds (Allen et al., 2008). The degree to which a cloud can form a group or association of stars is majorly governed by the dense material in the molecular cloud (Lada and Lada, 2003). The star formation scenario and the physical processes affecting the star formation in the region can be well understood by the mapping of young stellar objects (YSOs; Koenig et al. 2008). Various surveys of molecular clouds reveal that approximately 75% of the embedded young stars exist in groups their clusters have equal to or more than 10 members (Zinnecker et al., 1993; Allen et al., 2007). The quantitative structural analysis of these clusters; the sizes, densities, and morphologies of young stellar cores: can be used to examine the theoretical models of star formation (Kuhn et al., 2014).

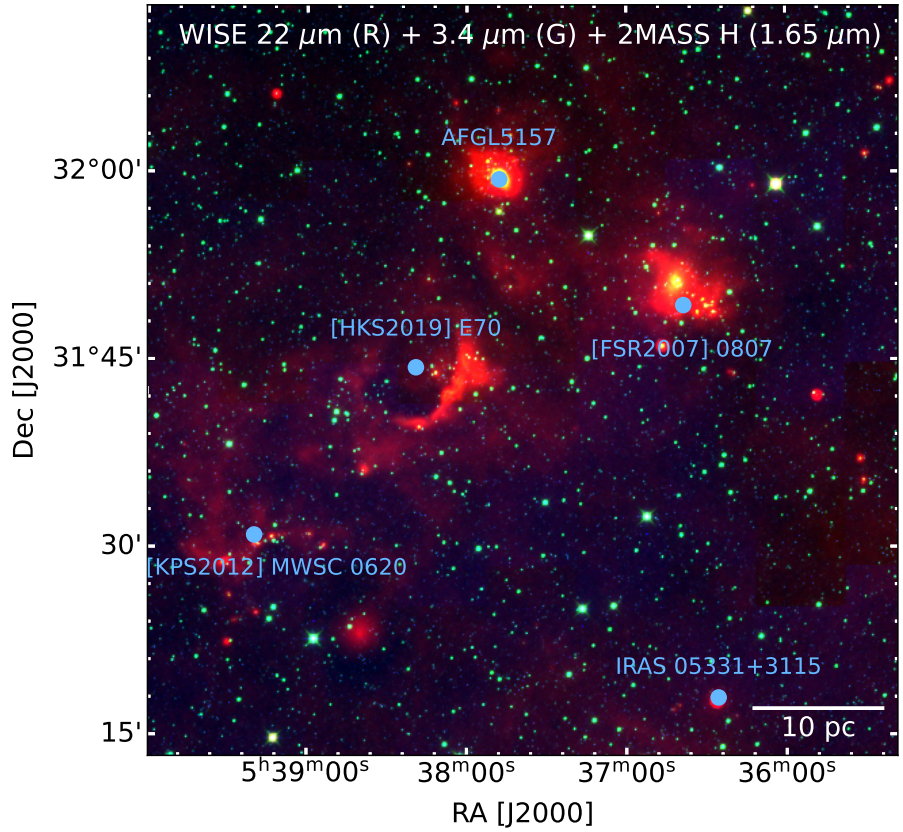

Figure 1: Color-composite image (Red: *WISE* 22 μm; Green: *WISE* 3.4 μm; Blue: 2MASS H band, 1.65 μm) of $1^\circ \times 1^\circ$ region overlaid with the locations of five clusters (blue circle).

2. Source Selection

Active star-forming regions in molecular clouds generally consist of young star clusters (YSCs), mid-infrared (MIR) bubbles, clouds/filaments, and massive stars. Previous studies have suggested that the expansion of bubbles associated with the H II regions can trigger 14 to 30% of the formation of the stars (e.g., Deharveng et al. 2010, Kendrew et al. 2012).

For the present study, we have selected a poorly explored region of $1^\circ \times 1^\circ$ which consists of five clusters: AFGL 5157 ($\alpha = 05^{\rm h}\,37^{\rm m}\,48^{\rm s}$ and $\delta = +31^\circ 59' 44''$), MIR bubble [HKS2019] E70 ($\alpha = 05^{\rm h}\,38^{\rm m}\,19^{\rm s}$ and $\delta = +31^\circ 44' 22''$), [FSR2007] 0807 ($\alpha = 05^{\rm h}\,36^{\rm m}\,39^{\rm s}$ and $\delta = +31^\circ 49' 20''$), [KPS2012] MWSC 0620 ($\alpha = 05^{\rm h}\,39^{\rm m}\,20^{\rm s}$ and $\delta = +31^\circ 30' 58''$) and an H II region IRAS 05221+3115 ($\alpha = 05^{\rm h}\,36^{\rm m}26^{\rm s}$ and $\delta = +31^\circ 17' 43''$).

Figure 1 shows the color-composite image (Red: *WISE* 22 μm; Green: *WISE* 3.4 μm; Blue: 2MASS H band, 1.65 μm) of $1^\circ \times 1^\circ$ region overlaid with the locations of five clusters (blue color). The *WISE* 22 μm represents the distribution of warm gas. The MIR emission in 3.4 μm wavelength indicates the distribution of gas and dust. All these features coincide with the locations of identified clusters indicating strong evidence of star formation activities.

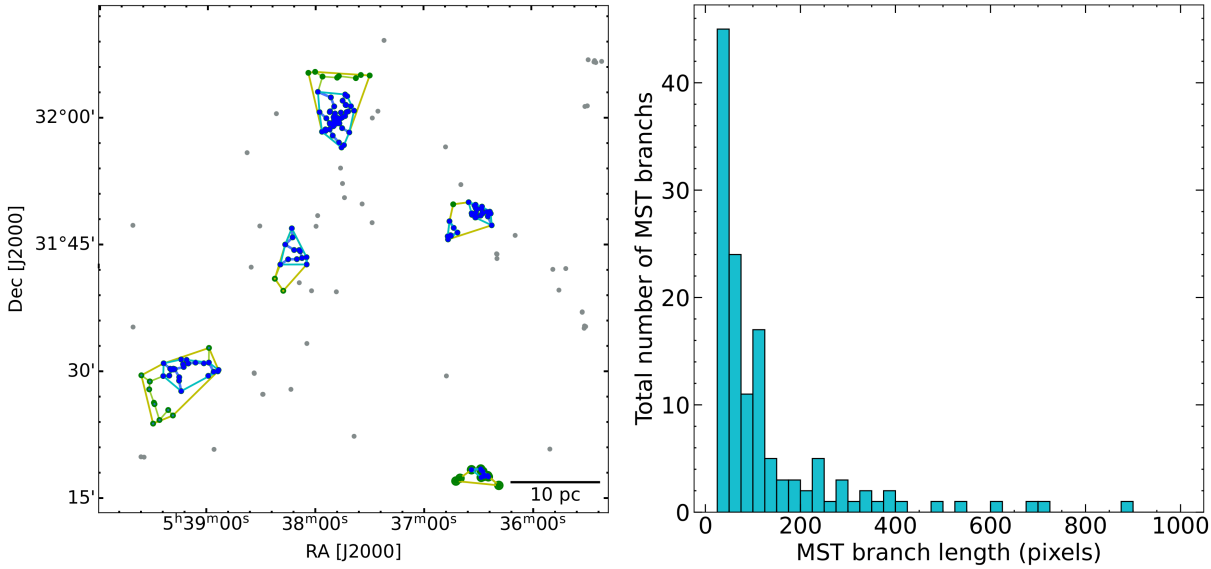

Figure 2: (left) MST connections in the core (blue) and AR (green) and the locations of YSOs (blue dots for the YSOs in the core and green dots for the YSOs in AR). The isolated cores and ARs are also enclosed by the *Convex hulls* using cyan and yellow lines, respectively. The locations of the identified YSOs are also marked by black dots. (right) Histogram of the MST branch lengths.

3. Extraction of the Cores and the Active Regions (ARs)

Assuming that the five clusters in the region might be fragmented from the same molecular cloud, we isolated them by applying an empirical technique *'Minimal Spanning Tree'* (MST; Gutermuth et al. 2009). This technique finds edges with minimum weight in each iteration and then adds them to the MST. The advantage of this technique is that it isolates the subgroups without biasing or smoothening and prevents basic geometry (Cartwright and Whitworth, 2004; Gutermuth et al., 2009; Pandey et al., 2020). We used this technique on the identified YSOs based on excess IR emission. The MST is plotted in the left panel of Fig. 2, which points towards five subgroups in the region having different concentrations of YSOs. The dots and lines in different colors are representing the YSOs and the MST branches, respectively. We chose a surface density threshold stated as critical branch length to isolate the subgroups by plotting a histogram between MST branch lengths and MST branch numbers (right panel of Fig. 2). The histogram peaks at a relatively small spacing than large spacing which indicates the existence of significant subgroups. If the sources have a branch length less than the critical branch length, then they are considered part of the same cluster.

These sub-groups are enclosed by selecting a point where the shallow-sloped segment has a gap in the distribution of MST branch lengths. These regions are termed as 'active regions' (AR). It is considered that these regions have moved out of the core (overdense regions) because of dynamic evolution. The critical branch lengths are 100 and 125 pixels for the cores and ARs, respectively. The YSOs and MST connections in the cores and ARs are represented by blue and green dots and lines, respectively, in the left panel of Fig. 2. The isolated cores and ARs

Table 1: Properties of the Identified Cores and ARs. We list central position of the sub-regions (Region), the total number of enclosed YSOs ($N_{\rm tot}$), the number of enclosed Class I YSOs ($N_{\rm I}$), the number of enclosed Class II YSOs ($N_{\rm II}$), the number of the vertices of the convex hull (V), the radius of the cluster ($R_{\rm cluster}$), the circle radius ($R_{\rm circ}$), the aspect ratio and the Q parameter.

Region	$N_{\rm tot}$	$N_{\rm I}$	$N_{\rm II}$	V	$R_{\rm cluster}$ (pc)	$R_{\rm circ}$ (pc)	**Aspect Ratio**	Q **parameter**
For Cores								
AFGL5157	52	2	50	9	2.62	3.39	3.96	0.62
[HKS2019] E70	12	0	12	5	2.59	2.19	0.71	0.50
[FSR2007] 0807 (C1)	16	4	20	7	1.29	1.82	2.00	0.55
[FSR2007] 0807 (C2)	7	2	5	4	0.89	1.02	1.31	0.44
[KPS2012] MWSC 0620	25	5	20	9	2.61	3.10	1.41	0.39
IRAS 05221+115	10	0	10	5	0.75	2.00	7.17	0.24
For ARs								
AFGL5157	60	2	58	7	3.57	4.58	1.64	0.38
[HKS2019] E70	15	1	14	6	2.59	3.53	1.86	0.81
[FSR2007] 0807	30	5	25	9	2.56	2.80	1.20	0.61
[KPS2012] MWSC 0620	36	10	26	7	3.95	5.27	1.78	0.37
IRAS 05221+115	13	3	9	4	1.44	2.77	3.70	0.23

are enclosed by the *Convex hulls* using cyan and yellow lines, respectively. All the clusters are found to have a single core, whereas [FSR2007] 0807 is found to have two cores which are termed C1 and C2. The locations of all the identified YSOs are shown by black dots. We have also calculated the radius of the cores and ARs ($R_{\rm cluster}$), $R_{\rm circ}$, and aspect ratio. $R_{\rm circ}$ is expressed as half of the distance between the two most distant hull points, whereas the aspect ratio is $\frac{R^2_{\rm circ}}{R^2_{\rm cluster}}$. The evaluated parameters of identified regions are given in Table 1.

The shape of the cluster may not always be circular. So, the cluster area is redefined by *convex hull*, which is a polygon enclosing all points of a grouping with internal angles less than 180° between two contiguous sides (Schmeja and Klessen 2006, Sharma et al. 2020). The *convex hull* is used to evaluate the area of the cluster $A_{\rm cluster}$ (Sharma et al., 2020), given as:

$$A_{\rm cluster} = \frac{A_{\rm hull}}{1 - \frac{n_{\rm hull}}{n_{\rm total}}}$$

where $A_{\rm hull}$ is the hull area, $n_{\rm hull}$ is the total number of hull vertices and $n_{\rm total}$ is the number of points lying inside the hull. $R_{\rm cluster}$ is the radius of the circle whose area is equal to $A_{\rm cluster}$.

4. Result and Conclusion

We examined the spatial distribution of the YSOs in the $1^\circ \times 1^\circ$ region near the star-forming site AFGL 5157. MST analysis of the region reveals the presence of five major clustering in the

region. We have determined the basic structural parameters of these regions and found that the radius of the cluster varies between 0.75 pc to 2.62 pc with a mean value of 1.74 pc. In contrast, the aspect ratio varies between 0.71 to 7.17. Thus this region consists of clumpy as well as elongated clusters. We also calculated structure parameter Q for each region (see Table 1) and found that it varies between 0.41-0.62 and 0.23-0.81 for the cores and ARs, respectively. The large Q values (i.e., > 0.8) are related to the centrally condensed spatial distributions, whereas small Q values (i.e., < 0.8) are related to the fractal substructures (Dib and Henning, 2019). This shows the existence of fractal distribution in all the cores and ARs except the core of [HKS2019] E70. Since [HKS2019] E70 has $Q > 0.8$, thus it has a centrally condensed spatial distribution.

Acknowledgments

This publication makes use of data from the Two Micron All Sky Survey, which is a joint project of the University of Massachusetts and the Infrared Processing and Analysis Center/California Institute of Technology, funded by the National Aeronautics and Space Administration and the National Science Foundation. This work is based on observations made with the *Spitzer* Space Telescope, which is operated by the Jet Propulsion Laboratory, California Institute of Technology under a contract with the National Aeronautics and Space Administration. This publication makes use of data products from the Wide-field Infrared Survey Explorer, which is a joint project of the University of California, Los Angeles, and the Jet Propulsion Laboratory/California Institute of Technology, funded by the National Aeronautics and Space Administration. A.V. acknowledges the financial support of DST-INSPIRE (No.: DST/INSPIRE Fellowship/2019/IF190550).

Further Information

Authors' ORCID identifiers

0000-0002-6586-936X (Aayushi VERMA)
0000-0001-5731-3057 (Saurabh SHARMA)
0000-0001-6725-0483 (Lokesh DEWANGAN)

Author contributions

The present study results from a collaboration to which all the authors have significantly contributed.

Conflicts of interest

The authors declare no conflict of interest.

References

Allen, L., Megeath, S. T., Gutermuth, R., Myers, P. C., Wolk, S., Adams, F. C., Muzerolle, J., Young, E. and Pipher, J. L. (2007) The structure and evolution of young stellar clusters. In Protostars and Planets V, edited by Reipurth, B., Jewitt, D. and Keil, K., p. 361. https://doi.org/10.48550/arXiv.astro-ph/0603096.

Allen, T. S., Pipher, J. L., Gutermuth, R. A., Megeath, S. T., Adams, J. D., Herter, T. L., Williams, J. P., Goetz-Bixby, J. A., Allen, L. E. and Myers, P. C. (2008) *Spitzer*, near-infrared, and submillimeter imaging of the relatively sparse young cluster, Lynds 988e. ApJ, 675(1), 491–506. https://doi.org/10.1086/525241.

Cartwright, A. and Whitworth, A. P. (2004) The statistical analysis of star clusters. MNRAS, 348(2), 589–598. https://doi.org/10.1111/j.1365-2966.2004.07360.x.

Deharveng, L., Schuller, F., Anderson, L. D., Zavagno, A., Wyrowski, F., Menten, K. M., Bronfman, L., Testi, L., Walmsley, C. M. and Wienen, M. (2010) A gallery of bubbles. The nature of the bubbles observed by spitzer and what ATLASGAL tells us about the surrounding neutral material. A&A, 523, A6. https://doi.org/10.1051/0004-6361/201014422.

Dib, S. and Henning, T. (2019) Star formation activity and the spatial distribution and mass segregation of dense cores in the early phases of star formation. A&A, 629, A135. https://doi.org/10.1051/0004-6361/201834080.

Gutermuth, R. A., Megeath, S. T., Myers, P. C., Allen, L. E., Pipher, J. L. and Fazio, G. G. (2009) A *Spitzer* survey of young stellar clusters within one kiloparsec of the Sun: Cluster core extraction and basic structural analysis. ApJS, 184(1), 18–83. https://doi.org/10.1088/0067-0049/184/1/18.

Kendrew, S., Simpson, R., Bressert, E., Povich, M. S., Sherman, R., Lintott, C. J., Robitaille, T. P., Schawinski, K. and Wolf-Chase, G. (2012) The Milky Way project: A statistical study of massive star formation associated with infrared bubbles. ApJ, 755(1), 71. https://doi.org/10.1088/0004-637X/755/1/71.

Koenig, X. P., Allen, L. E., Gutermuth, R. A., Hora, J. L., Brunt, C. M. and Muzerolle, J. (2008) Clustered and triggered star formation in W5: Observations with *Spitzer*. ApJ, 688(2), 1142–1158. https://doi.org/10.1086/592322.

Kuhn, M. A., Feigelson, E. D., Getman, K. V., Baddeley, A. J., Broos, P. S., Sills, A., Bate, M. R., Povich, M. S., Luhman, K. L., Busk, H. A., Naylor, T. and King, R. R. (2014) The spatial structure of young stellar clusters. I. subclusters. ApJ, 787(2), 107. https://doi.org/10.1088/0004-637X/787/2/107.

Lada, C. J. and Lada, E. A. (2003) Embedded clusters in molecular clouds. ARA&A, 41, 57–115. https://doi.org/10.1146/annurev.astro.41.011802.094844.

Pandey, R., Sharma, S., Panwar, N., Dewangan, L. K., Ojha, D. K., Bisen, D. P., Sinha, T., Ghosh, A. and Pandey, A. K. (2020) Stellar cores in the Sh 2-305 H II region. ApJ, 891(1), 81. https://doi.org/10.3847/1538-4357/ab6dc7.

Schmeja, S. and Klessen, R. S. (2006) Evolving structures of star-forming clusters. A&A, 449(1), 151–159. https://doi.org/10.1051/0004-6361:20054464.

Sharma, S., Ghosh, A., Ojha, D. K., Pandey, R., Sinha, T., Pandey, A. K., Ghosh, S. K., Panwar, N. and Pandey, S. B. (2020) The disintegrating old open cluster Czernik 3. MNRAS, 498(2), 2309–2322. https://doi.org/10.1093/mnras/staa2412.

Zinnecker, H., McCaughrean, M. J. and Wilking, B. A. (1993) The initial stellar population. In Protostars and Planets III, edited by Levy, E. H. and Lunine, J. I., p. 429.